Appl. Phys. A 81, 399–404 (2005)
DOI: 10.1007/s00339-004-2601-6

Applied Physics A
Materials Science & Processing

U. BERNINI[1]
R. BERNINI[2]
P. MADDALENA[1,✉]
E. MASSERA[1]
P. RUCCO[1]

Determination of thermal diffusivity of suspended porous silicon films by thermal lens technique

[1] INFM, Dipartimento di Scienze Fisiche, Università di Napoli "Federico II", Complesso Universitario di Monte S. Angelo, Via Cintia, 80126 Napoli, Italy
[2] C.N.R. – IREA, Via Diocleziano 328 - 1, 80124 Napoli, Italy

Received: 9 July 2003 /Accepted: 14 January 2004
Published online: 16 March 2004 •

ABSTRACT In this paper, the thermal diffusivity of free-standing films of nanoporous silicon has been studied. The films were obtained by electrochemical etching of *p*-type silicon. Measures were performed under vacuum and in the temperature range 300–600 K, so that the internal sample surface was not contaminated by ambient pollutants and hydrogen desorption did not affect significantly the surface chemistry due to high temperature effects. An investigation technique, based on thermal lensing, was adopted since it seemed to be more suitable than other techniques generally used for the determination of thermal properties of porous layers on crystalline substrates. The comparison between theoretical previsions and experimental results obtained for thin layers of known properties shows that the developed technique is reliable and of easy application for solid samples of low thermal conductivity. The diffusivity of the investigated nanoporous silicon samples is reduced with respect to the one of crystalline silicon due to both the porosity of the material and to the reduction in diffusivity of each individual nanocrystal, resulting from the enhanced boundary scattering of lattice waves.

PACS 78.20.Nv; 44.30.+v; 42.65.Jx; 68.60.Dv

1 Introduction

A recent, largely diffuse manner of obtaining materials with new properties is represented by the reduction of materials, whose properties are well known, in particles of dimensions so small that the contribution of surface effects strongly affects their physical properties [1].

A typical example is represented by porous silicon (PS), in which both the chemical state of its extended surface and the Si skeleton reduced dimensions influence the optical, electric and thermal properties of the system [2].

However, the knowledge of the thermo physical properties of these materials, often produced as thin films, is generally important for their use in the technological field.

In the case of PS, recently reported measurements of thermal conductivity of PS layers on crystalline substrate show that for nanocrystalline structures (nanoporous silicon) formed on *p*-type Si, the conductivity is very low with respect to the one of bulk Si at ambient temperature ($150\ \mathrm{Wm^{-1}\,K^{-1}}$): in high porous layers (porosity $\cong 80\%$), it is of the same order of magnitude [3, 4] than the conductivity of air ($0.026\ \mathrm{Wm^{-1}\,K^{-1}}$).

It is, then, evident that thermal analysis of such materials requires a proper choice of both the method and conditions of measurement.

Indeed, contact intrusive methods or atmospheric impregnation [5] may induce a sample contamination and an alteration of its chemical composition that may alter the measurement results.

The aim of this work is the measurement of the thermal diffusivity of free standing samples of nano-PS. Measurements have been performed in vacuum and in the thermal range between 300 and 600 K, in such a way that the samples did not contain residual water, which could hardly be removed by normal drying, and avoiding alteration of the chemical surface conditions due to hydrogen desorption, whose onset is at $T > 500$ K in high vacuum [6].

The investigation method is a simplified version of a technique based on thermal lensing (TL). Indeed, various methods have been proposed in the literature for the measurement of either the conductivity or the thermal diffusivity of porous silicon layers on crystalline substrate [3, 4, 7–12].

These methods, however, seem to be inadequate or, at least, of difficult application to the analysis of thin suspended films. Techniques such as the photoacustic technique [7] or the photothermal deflection technique [8] based on the mirage effect [11] require that the sample be immersed in a coupling fluid, so that under vacuum measurements are practically impossible. Moreover, in these methods the sample is heated by an intensity modulated laser beam, which induces in the suspended film thermoelastic vibrations that cannot be neglected. Thus, even working under inert gas conditions instead of vacuum, long lasting measurements are required, that normally are also of complicated interpretation.

The use of microdevices [3, 9] for the generation of thermal waves, whose propagation in the porous layer is then analyzed, introduces in our case contact and stability problems that cannot be overcome. More adequate appear the optical methods based on micro-Raman spectroscopy [12] or on the time decay of the transmittance of a probe beam, induced by transient heating due to a pump pulse [10]. Even these techniques suffer from some limitations: the former re-

✉ Fax: +39-81/676346, E-mail: maddalena@na.infn.it

quires the use of focused beams, since it gives accurate results only for samples whose thickness is greater than the incident beam diameter, the latter has a limitation in the sample degradation due to the prolonged exposure to high intensity light pulses.

The method proposed by us, as all the mentioned techniques, has both advantages and disadvantages: however, it allows for a reliable and immediate determination of thermal diffusivity of thin film materials, not necessarily of porous structure.

In a TL based experiment, a pump beam, of Gaussian intensity distribution, induces in a lightly absorbing sample a radial refractive index gradient, thus creating a "thermal lens". This fact influences the propagation of a probe beam, which is collinear to the pump one.

An evaluation of thermal diffusivity can be obtained by time resolved measures of the intensity variation at the center of the probe beam [13], since the intensity variations are correlated to the phase shift, that is induced by TL on the probe beam and that depends on the thermal time constant of the material.

Unfortunately, the expression relating the intensity variation to conductivity involves parameters, which are not a priori known as in our case.

Our measurements have been performed using an unfocused Gaussian pump beam and an incoherent uniform probe beam, whose dimensions are about the same of the pump beam.

For thin samples (tens of μm) and at low irradiating intensities, the induced TL effect generates a perfect thin lens. Any residual spherical aberration has an insignificant effect over a probe beam of the same dimensions [14]. In these conditions, instead of probing the central region of the heated zone, it is possible to probe the region in which the refractive index gradient is maximum at the advantage of the technique sensitivity.

Simple considerations based on geometrical optics lead to a relation that allows direct determination of thermal diffusivity of the medium.

A comparison between previsions and experimental results for samples of known diffusivity confirms the method validity.

Thermal conductivity deduced for the analyzed freestanding PS samples from diffusivity data is in agreement with values reported in literature for analogous samples on crystalline substrates, analyzed in the same physical conditions (under vacuum) [3].

Obtained results confirm the expectation that heat transfer occurs only through the Si skeleton and that the diffusivity, of the solid component, is mainly determined by the mean free path of phonons in silicon nanocrystallites.

2 Theory

Let us suppose a Gaussian laser beam, propagating along z direction, is normally incident on a thin absorbing layer. If the medium thickness l along the propagation direction is small with respect to the laser spot radius R, then $\tau_l = l^2 4D \ll R^2 4D = \tau$, where τ_l and τ are the longitudinal and radial diffusion time constants, respectively, $D = K/\varrho c$ is the diffusivity, K is the conductivity and (ϱc) the medium heat capacity for unit volume.

Under this hypothesis, the term containing $\partial^2 T/\partial z^2$ can be neglected in the heat equation. Neglecting convection losses, too (the sample is under vacuum) and under the hypothesis that transverse dimensions of the sample are much greater than the spot radius, the temperature distribution is obtained by solving the equation:

$$\frac{1}{r}\frac{\partial}{\partial r}\left(r\frac{\partial T}{\partial r}\right) = \frac{1}{D}\frac{\partial T}{\partial t} - \frac{\beta}{K} I_0 \,\mathrm{e}^{-r^2/R^2}\mathrm{e}^{-\beta z}, \tag{1}$$

where I_0 is the incident beam intensity and β is the optical absorption coefficient.

The solution of (1), obtained adopting the Hankel transforms method [15], is given by:

$$T = \frac{\beta I_0 \mathrm{e}^{-\beta z}}{K}\frac{R^2}{2}\int_0^\infty \left(\frac{\mathrm{e}^{-R^2\varrho^2/4}}{\varrho} - \frac{\mathrm{e}^{-R^2\varrho^2(1+t/\tau)/4}}{\varrho}\right) J_0(r\varrho)\mathrm{d}\varrho, \tag{2}$$

where $\frac{R^2}{2}\mathrm{e}^{-R^2\varrho^2/4}$ is the 0 order Hankel transform of e^{-r^2/R^2} and J_0 the 0 order Bessel function of first kind.

Since, for the Bessel functions properties [16] $\frac{\partial}{\partial r}J_0(r\varrho) = -\frac{\varrho^2}{r}\int_0^r r' J_0(r'\varrho)\mathrm{d}r'$, the radial temperature gradient $\partial T/\partial r$ is given by:

$$\frac{\partial T}{\partial r} = \frac{\beta P \mathrm{e}^{-\beta z}}{2\pi K}\frac{1}{r}\left(\mathrm{e}^{-r^2/R^2} - \mathrm{e}^{-r^2/R^2(1+t/\tau)}\right) \tag{3}$$

where P is the pump beam power.

Equation (3) has been derived ignoring self-focusing or defocusing effects of the pump beam inside the sample; these phenomena, due to the low powers used and to the small sample thickness, are, indeed, negligible.

Let us now consider a probe beam, incoherent and spatially uniform of intensity I_0', which is superimposed to the pump beam and has about the same transverse dimensions. The deflection φ, at the sample output undergone by that part of the beam at a distance r from the axis for small angular deflections is given by [17]:

$$\begin{aligned}\varphi &= \frac{1}{n}\frac{\partial n}{\partial T}\int_0^l \frac{\partial T}{\partial r}\mathrm{d}z \\ &= \frac{P\left(1-\mathrm{e}^{-\beta l}\right)}{2\pi K}\frac{1}{n}\frac{\partial n}{\partial T}\frac{1}{r}\left(\mathrm{e}^{-r^2/R^2} - \mathrm{e}^{-r^2/R^2(1+t/\tau)}\right)\end{aligned} \tag{4}$$

where $\frac{1}{n}\frac{\partial n}{\partial T}$ is the thermal coefficient of the refractive index.

The deflection angle, for $t > 0$, reaches its maximum value in correspondence of the flex point of temperature distribution $\left(\partial^2 T/\partial r^2 = 0\right)$ and it is more or less pronounced depending if t is greater or smaller than τ. If $t > \tau$, φ reaches its maximum when $r/R \approx 1$; if, on the contrary, $t < \tau$ the maximum is reached for $r/R < 1$ (as an example, if $t = 10^{-3}\tau$, $r/R \approx 0.7$; in this case, however, around $r/R = 1$ variations of φ are very small since the behavior is flat (see Fig. 1).

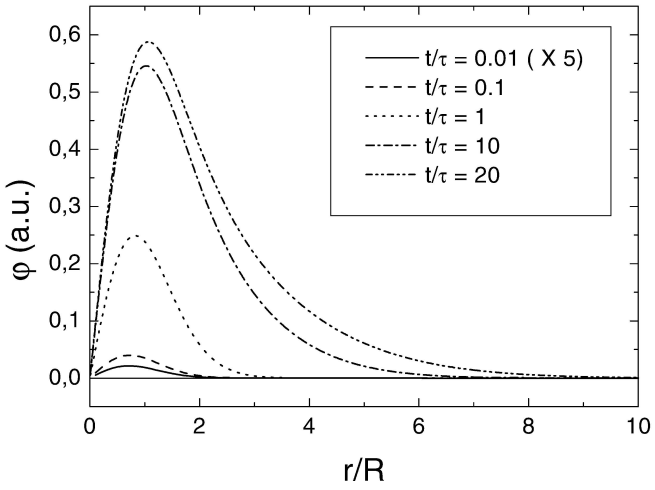

FIGURE 1 Behaviour of the deflection angle φ as function of the ratio r/R for different values of t/τ

Consequently, all the rays, traveling at a distance $r = R \pm \mathrm{d}R$ from the axis with $\mathrm{d}R \ll R$, undergo the same deflection, for varying time, since they are in a region where φ variations are small.

In Fig. 2 φ is reported (at less of a multiplicative factor $\ll 1$) as function of t/τ, for $r/R = 0.95, 1.00, 1.05$. We observe that for $\mathrm{d}R/R = 5 \times 10^{-2}$ in stationary conditions $(t \gg \tau)\ \mathrm{d}\varphi/\varphi < 6 \times 10^{-3}$.

Once the ray deflection and its position r at the sample output are known, the ray position at a distance L is given by $r \pm L\varphi$ accordingly, if defocusing or focusing of the probe beam occurs, where L is the coordinate of the observation plane. In this plane, let us put a diaphragm, whose aperture has a radius R and a photomultiplier behind it; then, under the condition $L\bar{\varphi} \ll R$,where $\bar{\varphi} = \varphi_{r=R}$, the power variation measured by the photomultiplier is given, at a good approximation, by $2\pi R I_0'(L\bar{\varphi})$. In stationary conditions, for $L\bar{\varphi} = 0.05R$, the power variation is $0.1\pi R^2 I_0'$, that is 10% of the power measured in absence of the pump beam, so it is easily detectable.

We verified that condition $L\bar{\varphi} \ll R$ is fulfilled for many solid samples. In solids, indeed, $\frac{1}{n}\frac{\partial n}{\partial T}$ is typically $10^{-4} \sim 10^{-5} K^{-1}$. We derived an estimation of this coefficient (unpublished measurements) with an interferometric laser technique [18] for nano-PS layers on crystalline substrate, fabricated from p-type Si of variable porosity between 43% and 61% in a temperature range from 300 to 700 K. In the calculation, thermal expansion effects [19] have been neglected, and for the refractive index, we have used the value of $n = 1.9$ at $\lambda = 633$ nm, deduced from reflectance measurements, in similar samples, by Kramers–Kronig analysis [20]. Obtained results show that, for a sample of $\approx 50\%$ porosity, the average value of $\frac{1}{n}\frac{\partial n}{\partial T}$ in the examined thermal range is $\approx 1.1 \times 10^{-4}\ \mathrm{K}^{-1}$, that is of the order of magnitude typical of solids.

Since, in our apparatus, $R = 0.8$ mm and L variable between 50 and 10^3 mm, even for very low values of thermal conductivity ($K = 0.02\ \mathrm{Wm}^{-1}\ \mathrm{K}^{-1}$) the condition $L\bar{\varphi} \ll R$ can be satisfied by a proper choice of L.

In Fig. 3 the behavior of $\bar{\varphi}$ (per milliwatt of absorbed light power) is shown as a function of thermal conductivity K, assuming $\frac{1}{n}\frac{\partial n}{\partial T} = 10^{-4} K^{-1}$. Since $\bar{\varphi}$ is directly proportional to $\frac{1}{n}\frac{\partial n}{\partial T}$, a simple multiplication of $\bar{\varphi}$ by a scale factor is needed to get the behavior at different values of $\frac{1}{n}\frac{\partial n}{\partial T}$. Condition $L\bar{\varphi} \ll R$, for example $L\bar{\varphi} \leq 0.05R$, is verified for the lowest value of K ($0.02\ \mathrm{Wm}^{-1}\ \mathrm{K}^{-1}$) when $L \leq 63$ mm.

If $K \geq 0.31\ \mathrm{Wm}^{-1}\ \mathrm{K}^{-1}$, the same condition holds whichever be the value of L in the allowed range of our experimental apparatus.

The relative variation of measured power $\Delta P/P$, per milliwatt of absorbed light power, with $K = 0.02\ \mathrm{Wm}^{-1}\ \mathrm{K}^{-1}$ and $L = 63$ mm, is 10%. In Fig. 4 we show the relative variation $\Delta P/P$ of the probe beam power, per milliwatt of absorbed pump beam power as function of thermal conductivity K, assuming $L = 10^3$ mm. $\Delta P/P$ decreases for increasing K: as an example at $K = 20\ \mathrm{Wm}^{-1}\ \mathrm{K}^{-1}$, the relative variation is $\approx 0.20\%$. This is an easy detectable limit, which can be even reduced adopting a lock-in detection technique, thus confirming the validity of the proposed method in the analysis of solids of low or medium conductivity. When materials of high conductivity and/or having low transmittance at the probe

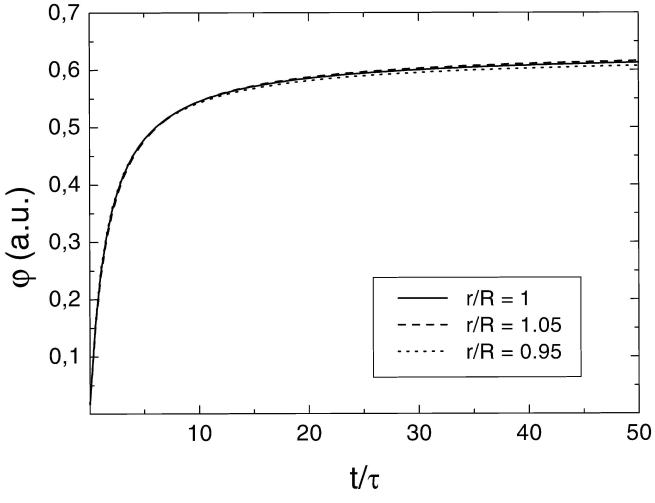

FIGURE 2 Behaviour of the deflection angle φ as function of t/τ for different values of the ratio r/R

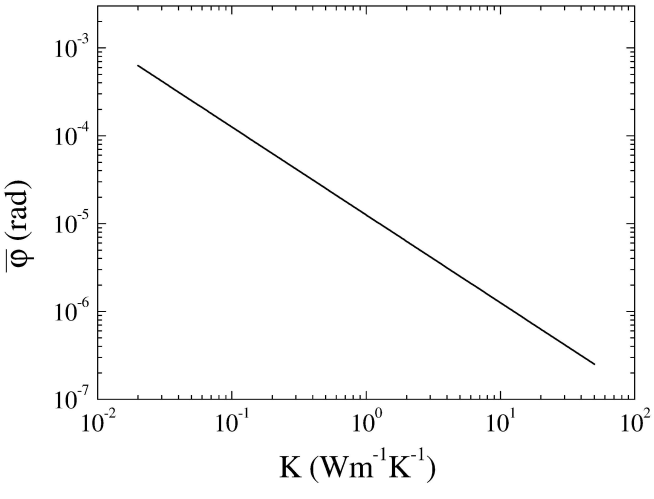

FIGURE 3 Behaviour of the deflection angle $\overline{\varphi}$ as function of conductivity K per milliwatt of absorbed light power, assuming $\frac{1}{n}\frac{\partial n}{\partial T} = 10^{-4}\ \mathrm{K}^{-1}$

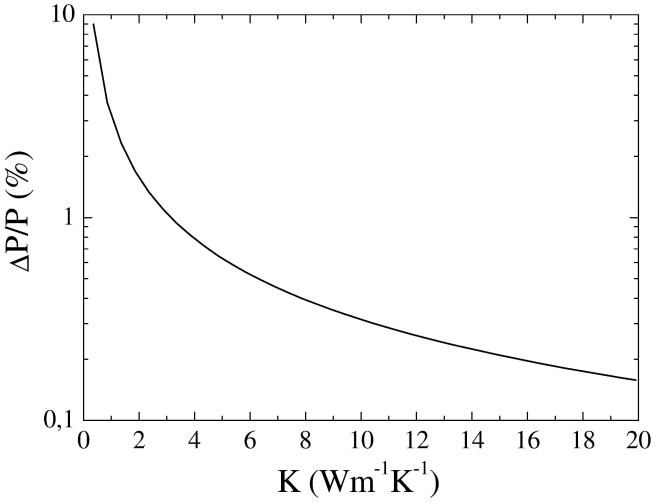

FIGURE 4 Relative variation $\Delta P/P$ of the probe beam power, per milliwatt of absorbed pump beam power, as function of thermal conductivity K, assuming $L = 10^3$ mm

wavelength are considered, the sensitivity of the method is reduced. Since we do not expect that a solid has a thermal conductivity less than 0.02 $\mathrm{Wm^{-1}\,K^{-1}}$, in our case, we adopted the practical criterion of verifying, at first, that the power variation at a given value of L was less than 10% of the power measured in absence of the pump beam; then, signal detection was performed by a lock-in technique, modulating the intensity of the incident probe beam.

Finally, since the detector signal is proportional to the incident power, it follows that:

$$\frac{\Delta P_t}{\Delta P_\infty} = \frac{\mathrm{e}^{-1} - \mathrm{e}^{-1/(1+t/\tau)}}{\mathrm{e}^{-1} - 1} = 1.58\,\mathrm{e}^{-1/(1+t/\tau)} - 0.58, \qquad (5)$$

where ΔP_t is the power variation measured at time t and ΔP_∞ is the power variation measured for $t \gg \tau$.

Comparison between experimental results and (5) allows determination of $\tau = R^2/4D$ and, hence, of the diffusivity D.

3 Experimental results and discussion

The experimental apparatus is shown in Fig. 5. Lenses L1, L2 and L3 form a collimating system for the radiation emitted by a LED ($\lambda_{\mathrm{peak}} = 640$ nm). The beam is expanded and spatially filtered by a pinhole placed between lenses L2 and L3; the diaphragm D1 selects only the on-axis fraction of the beam, so that the transmitted beam (the probe beam) has a uniform transverse intensity distribution. D2 is a diaphragm, whose aperture radius is equal to the pump beam (ILT mod. 6500AWC-00C $\mathrm{Ar^+}$ cw laser, $\lambda = 488$ nm) radius at $1/\mathrm{e}$ of the irradiance distribution. The beamsplitter BS recombines the two beams that are incident on the sample. A laser beam analyzer (SPIRICON Inc. mod. LBA-100A), placed just behind D1, allows for the determination of the transverse distribution of both beams: the probe beam distribution has a top-hat profile within 3% while the pump beam distribution is Gaussian within 2%. We notice, however, that the main contribution to the signal comes from the probe beam annulus of radius R, which undergoes a deflection due to the index gradient induced by the pump beam, so we expect that

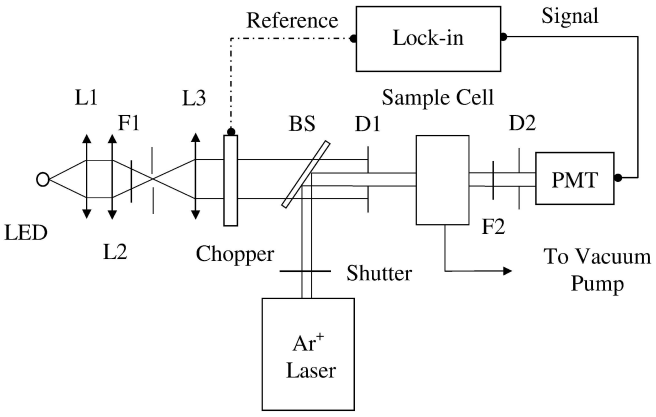

FIGURE 5 Experimental set-up

the assumption that the pump beam has a Gaussian shape, though allows for derivation of an analytical expression for the signal (5), has a relative weight on the detected signal.

The aperture radius of D1 is slightly greater than D2, so that either the focusing or defocusing of the probe beam can be detected by the photomultiplier (PMT). F1 and F2 are two interference pass-band filters ($\lambda = 633$ nm); the sample cell is a heating stage (MMR Technologies Inc. mod. R2300-27), containing the sample under investigation at an inner pressure of 20 mTorr.

The probe beam, which is incoherent to avoid unwanted interference phenomena in thin plates, is intensity modulated by a mechanical chopper for lock-in detection while a Pockels cell, whose rise-time is 20 ns, is used as a shutter for the pump beam.

Validity of the method has been checked analyzing samples of known diffusivity. In Fig. 6 we report the behavior of $\Delta P_t/\Delta P_\infty$ for a colored polymethylmethacrylate plate 300 μm thick, absorbing at $\lambda = 488$ nm and transparent at $\lambda = 633$ nm. The curve shown represents a fit of the experimental data by means of (5): the fitting procedure gives $\tau = (1.40 \pm 0.03)$s, corresponding to a thermal diffusivity $D = (1.14 \pm 0.02) \times 10^{-3}\,\mathrm{cm^2\,s^{-1}}$.

From data reported in literature for K [21], ϱ [22] and c [23], a diffusivity value of $1.15 \times 10^{-3}\,\mathrm{cm^2\,s^{-1}}$ is deduced;

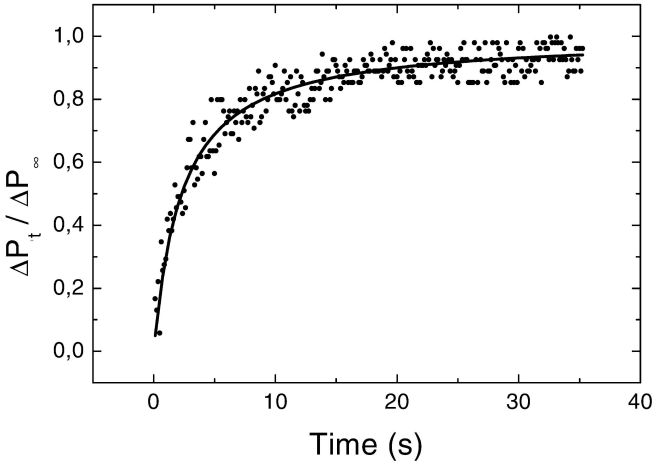

FIGURE 6 Time evolution of the normalized signal $|\Delta P_t|/|\Delta P_\infty|$, for a colored polymethylmethacrylate plate 300 μm thick

a direct comparison of data shows that the agreement is quite satisfactorily.

We, then, analyzed some freestanding PS samples, 18 μm thick, obtained from *p*-type Si, 1 Ω cm resistivity. The samples were fabricated by electrochemical etching in a water solution, containing 35% hydrofluoric acid and 30% isopropyl alcohol, at a current density of 13 mA/cm^2 and etching time of 15 min. A standard lift-off technique with a sudden increase in the current density was used to detach the porous membrane from the substrate. All samples have a structure made by an interconnected and homogeneous network of pores, with pore diameter and interpore spacing ≈ 4.9 nm, measured by SEM analysis, and porosity $\varepsilon \approx 50\%$, measured by a gravimetric method.

We, preliminarily, checked the possibility that the measured power variation could be caused by other phenomena, such as inverse saturation effects.

In principle, the small temperature increase, due to pump beam absorption, could induce a contraction of the PS bandgap and, consequently, an absorbance variation. Actually, by removing D2 diaphragm, so that the photomultiplier could detect all the transmitted power of the pump beam, the observed transmittance variation was negligible within the experimental errors.

In Fig. 7, the behavior of the effective thermal diffusivity, as a function of the temperature is reported for a sample, which has been investigated soon after the preparation (empty squares). The same behavior is reported for the same sample after three weeks, during which the sample was kept in dried air (filled squares).

Both behaviors are reproducible within the experimental errors, when the sample is subjected to cyclic variations of temperature: in Fig. 7 some data obtained during the cooling cycle of the aged sample are also reported (triangles).

In literature, a direct measurement of thermal diffusivity for samples similar to the investigated ones, is not reported; however, if the thermal capacity per unit volume for PS can be approximated by the relation $(\varrho c)_{\mathrm{PS}} = (1-\varepsilon)(\varrho c)_{\mathtt{crist}}$, it is possible to give an estimate of the effective conductivity K_{eff}.

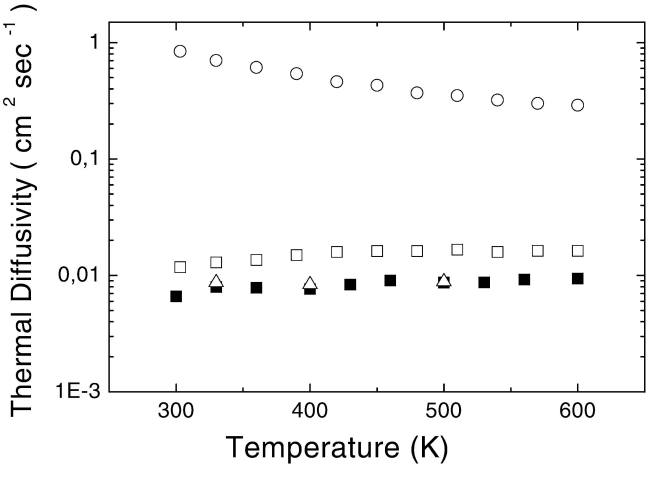

FIGURE 7 Effective thermal diffusivity D_{eff} as function of the temperature; *empty squares* refer to an as-prepared sample, *filled squares* to the same sample after three weeks, *triangles* to data obtained during the cooling cycle of the aged sample. *Empty circles* refer to the thermal diffusivity of crystalline silicon

At room temperature, $K_{\mathrm{eff}} \approx 0.9\,\mathrm{Wm^{-1}\,K^{-1}}$ for the as-prepared sample, that is, an intermediate value between the ones determined under vacuum conditions for porous layers on a crystalline substrate, similar to our samples, and whose porosity is 40% ($K_{\mathrm{eff}} = 1.2\,\mathrm{Wm^{-1}\,K^{-1}}$) [9] and 64% ($K_{\mathrm{eff}} = 0.2\,\mathrm{Wm^{-1}\,K^{-1}}$) [3].

We have also reported in the same figure, for sake of comparison, the behavior of crystalline Si diffusivity [24] in the same temperature range. In this range, indeed, the diffusivity of bulk Si is dominated by the phonon (lattice) contribution to conductivity and it decreases for increasing temperature, because of phonon–phonon scattering [20]. On the contrary, the effective diffusivity of PS is practically constant for both the as-prepared and aged samples, and it is about two orders of magnitude less than the bulk Si one.

To justify the low values found for both the conductivity and diffusivity of PS, different hypothesis have been formulated: Calderon et al. [25] determined the diffusivity behavior as a function of the etching time by a photoacustic technique for macroporous layers of *n*-type PS at room temperature and in ambient air.

By using a two-layer composite model, the solid phase conductivity was estimated to be close to the one of SiO_2 ($1.4\,\mathrm{Wm^{-1}\,K^{-1}}$) as if a high percentage of the oxide was present in the sample composition. However, as pointed out by the authors, the hypothesis needs to be verified, since, in that case, mainly the oxide should constitute the solid component.

Gesele et al. [3] using a technique based on electrically induced thermal waves propagation, determined the conductivity for *p*-type PS layers on a crystalline substrate between 35 and 320 K.

Since the measurements were performed under vacuum, the effective conductivity $\mathrm{K_{eff}}$ is the one of a medium made by a solid matrix, whose conductivity is K_{s}, and voids, whose conductivity is $K_{\mathrm{v}} = 0$.

In their model $K_{\mathrm{eff}} = (1-\varepsilon) g_0 K_{\mathrm{s}}$, where g_0 is a parameter representing the fraction of the interconnected solid phase, contributing to the conduction: according to the Looyenga model [26], they assume a porosity related expression for g_0 given by $g_0 = (1-\varepsilon)^2$.

The matrix conductivity is, then, expressed on the basis of a phenomenological model for phonon diffusion; if the phonons mean free path in each grain is Λ and l is the intrinsic mean free path, for $l > \Lambda$, one can then write:

$$K_{\mathrm{s}} = \frac{1}{3}\varrho c v \Lambda,$$

where v is the sound speed. Finally,

$$K_{\mathrm{eff}} = \frac{1}{3}(1-\varepsilon)^3 \varrho c v \Lambda, \tag{6}$$

where Λ is of the order of the grain size.

The authors find a good agreement between experimental results and (6) regarding both the temperature dependence, dominated by c, and the value of K_{eff}.

Lysenko et al. [27] adopted the same model of Gesele et al., to describe the thermal transport in as-prepared and oxidized nano-PS layers. To account for thermal transport in

the single nano-crystal, they introduced an effective scattering length, so that the phonons mean free path in the crystalline medium is given by:

$$\Lambda = \frac{l}{1+\frac{4}{3}\frac{l}{r}},$$

where r is the diameter of the nano-crystal, supposed spherical.

Adopting this model, since the thermal capacity per unit volume of nano-PS is approximated by $(1–\varepsilon)\varrho c$, the effective diffusivity $D_{\text{eff}} = \frac{K_{\text{eff}}}{(1-\varepsilon)(\varrho c)} = g_0 \frac{1}{3} v \Lambda$ is dependent on g_0 and Λ and is practically independent on temperature.

In our case, $r \approx 5$ nm; since $l \approx 40$ nm, we get $\Lambda \approx 3.4$ nm. Moreover $v = 6562\ \text{ms}^{-1}$ so that an estimation of D_{eff} can be given: $D_{\text{eff}} \approx 1.8 \times 10^{-2}\ \text{cm}^2\ \text{s}^{-1}$ in good agreement with experimental results (Fig. 7).

Also the diffusivity D_{eff} of the samples exposed to air and, hence, partially oxidized (Fig. 7) is rather independent on temperature over the investigated range, even if it is slightly lower than the one of as-prepared samples.

Data for D_{eff} after oxidation were not found in literature while the reported data for K_{eff} depend on the material, on the doping level and on the treatment. Lang et al. [28] reported a value slightly greater for the conductivity of a nano-PS sample prepared on lightly doped p-type Si after an oxidation process (300 °C, dry O_2 atmosphere, 1 h process duration). Measurements of the oxidized fraction distribution along the thickness for a similar sample show that the fraction is not negligible and is greater than 40% [27]. With such a high degree of oxidation, it is expected that the oxide layer gives a significant contribution to thermal transport, with a conductivity lower than the one of bulk Si, but the pore filling, due to oxidation induced expansion, may prevail since $K_{\text{eff}} \propto (1-\varepsilon)^3$ and may lead to a small increase in K_{eff}.

On the contrary, if the single crystal is covered by a very thin oxide layer, transport takes place preferably through the decreased Si cores and K_{eff} diminish. The preceding argumentation can be transferred to D_{eff} in view of the direct relation between conductivity and diffusivity, so the slight decrease of diffusivity we observed in p-type PS can be attributed to the reduced fraction of oxidized solid phase during storage in dry artificial air at ambient temperature, with respect to the one obtained in an oxidation process at 300 °C.

4 Conclusions

In this work, we measured the thermal diffusivity of freestanding PS samples, using a method based on TL effect. The proposed technique is a non-contact one and is characterized by the use of unfocused beams; this allows us to avoid difficulties, typical of TL spectroscopy, both in the careful alignment of the experimental setup and excessive local heating of the sample. As a consequence the apparatus results of easy assembly, the measurements are of easy derivation and their interpretation is not affected by the physics of the coupling fluid and thermoelastic phenomena.

Results, obtained for solid samples of known diffusivity, show that the adopted method is reliable and suitable for the analysis of thin suspended films even if it has unavoidable limitations. Indeed, the analysis can be performed on sample with low or medium conductivity, transparent to the probe beam. Moreover, the measurements are sensitive to intensity fluctuations of the probe beam.

For both the nano-porous samples analyzed soon after preparation and the partially oxidized ones, the effective diffusivity results are independent of temperature in the investigated range, and they are two orders of magnitude less than that of bulk crystalline Si. The effective conductivity, which is deduced from diffusivity measures, is in agreement with values reported in literature for samples obtained under the same conditions on crystalline substrate and analyzed under the same physical conditions.

Obtained results confirm the hypothesis that, analogously to what happens in polycrystalline solids, the low thermal diffusivity is due to the reduction in the diffusivity of each individual grain, resulting from the enhanced boundary scattering.

ACKNOWLEDGEMENTS The authors would like to thank G. Di Francia and V. La Ferrara at ENEA-CRIF, Portici (NA), Italy for fabrication of the PS samples.

REFERENCES

1 H. Gleiter: Progr. Mater. Sc. **33**, 223 (1989)
2 A.G. Cullis, L.T. Canham, P. Calcott: J. Appl. Phys. **82**, 909 (1997)
3 G. Gesele, J. Linsmeier, V. Drach, J. Fricke, R. Arens-Fischer: J. Phys. D: Appl. Phys **30**, 2911 (1997)
4 A.N. Obraztsov, V.Y. Timoshenko, H. Okushi, H. Watanabe: Semiconductors (U.SA.) **31**, 534 (1997)
5 L.T. Canham, M.R. Houlton, W.J. Leong, C. Pickering, J.M. Keen: J. Appl. Phys. **70**, 422 (1991)
6 S.M. Prokes, O.J. Glembocki, V.M. Bermudez, R. Kaplan: Phys. Rev. B **45**, 13 788 (1992)
7 G. Benedetto, L. Boarino, R. Spagnolo: Appl. Phys. A, **64**, 155 (1997); U. Bernini, P. Maddalena, E. Massera, A. Ramaglia: Opt. Commun. **168**, 305 (1999)
8 M. Bertolotti: Thin Solid Films **253**, 152 (1995)
9 A. Drost, P. Steiner, H. Moser, W. Lang: Sens. Mater. **7**, 111 (1995)
10 U. Bernini, S. Lettieri, P. Maddalena, R. Vitiello, G. Di Francia: J. Phys.: Condens. Matter **13**, 1141 (2001)
11 P.K. Kuo, E.D. Sendler, L.D. Favro, L. Thomas: Can. J. Phys. **64**, 1168 (1986)
12 S. Périchon, V. Lysenko, B. Remaki, D. Barbier, B. Champagnon: J. Appl. Phys. **86**, 4700 (19991)
13 J. Shen, R.D. Lowe, R.D. Snook: Chem. Phys. **165**, 385 (1992)
14 J. Shen, A.J. Soroka, R.D. Snook: J. Appl. Phys. **78**, 700 (1995)
15 H.S. Carsalaw, J.C. Jaeger: *Conduction of heat in solids* (Oxford, Clarendon, 1959)
16 A. Papoulis: *Systems and Tranforms with applications in Optics* (McGraw-Hill, 1968)
17 W.B. Jackson, N.M. Amer, C. Boccara, D. Fournier: Appl. Opt. **20**, 1333 (1981)
18 G. Abbate, A. Attanasio, U. Bernini, E. Ragozzino, F. Somma: J. Phys. D: Appl. Phys. **9**, 1945 (1976)
19 C. Faivre, D. Bellet, G. Dolino: J. Appl. Phys. **87**, 2131 (2000)
20 F. De Filippo, C. de Lisio, P. Maddalena, G. Lérondel, C. Altucci: Appl. Phys. A **73**, 737 (2001).
21 K. Eiermann: Kolloid Z. **198**, 5 (1964)
22 W.G. Gall, N.G. Mc Crum: J. Polym. Sci. **50**, 489 (1961)
23 R. Hoffmann, W. Knappe: Kolloid. Z. **247**, 763 (1971)
24 H.R. Shanks, P.D. Maycock, P.H. Sioles, G.C. Danielson: Phys. Rev. **130**, 1743 (1963)
25 A. Calderon, J.J. Alvarado-Gil, Y.G. Gurevich, A. Cruz-orea, I. Delgadillo, M. Vargas, L.C. Miranda: Phys. Rev. Lett. **79**, 5022 (1997)
26 H. Looyenga: Physica **31**, 401 (1965)
27 V. Lysenko, P.M. Roussel, B. Remaki, G. Delhomme, A. Dittmar, D. Barbier, V. Strikm, C. Martelet: J. Porous Mat. **7**, 177 (2000)
28 W. Lang: Thermal conductivity of Porous Silicon, *Properties of Porous Silicon*, ed. by L. Canham, EMIS Datareview Series, N. 18, p. 138 (Inspec, London 1997)